SELECTIVE TRANSDUCTION OF WINE-GLASS VIBRATION MODE USING DIFFERENTIAL OPTOMECHANICS

M.J. Storey[1], A.K. Bhat[1], and S.A. Bhave[2]
[1]OxideMEMS Lab, Cornell University, Ithaca, NY, USA
[2]Analog Devices, Woburn, MA, USA

ABSTRACT

This paper demonstrates differential optomechanical transduction which selectively drives and senses the wine-glass vibration mode of a silicon resonator. Two waveguide arms are used for optomechanical sensing at the anti-nodes of the 22 MHz wine-glass mode and utilize a differential photo detector (PD) to measure the vibration. The differential sense scheme enhances the wine-glass signal by 5.4 dB while significantly attenuating the radial "common-mode" vibration at 96.2 MHz by 11 dB.

KEYWORDS

Optomechanics, wine-glass mode, MEMS, differential transduction.

INTRODUCTION

Optomechanical transduction of a ring resonator is more sensitive to "path-length" change compared to "gap-change", making it easier to measure circumference change of the radial vibration mode instead of the gap-changing characteristic of wine-glass vibration mode [1, 2]. Tallur et al demonstrated that the f-Q product of wine-glass modes was larger than radial modes, but their transmission signal-levels were significantly smaller [3]. Differential gap-change has been implemented in macro-scale sensing such as LIGO [4], but has never been demonstrated at the chip-scale due to challenges associated with achieving critical optical coupling of two optical sensors to a micromechanical resonator.

This work presents the theory behind a two waveguide chip-scale differential optomechanical sensing scheme for a given mechanical mode. The fabrication and design of the 3-coupled ring resonator (as shown in figure 1) is described along with the experimental setup for fully differential electrostatic drive and differential optomechanical sensing. Experimental data is presented comparing the transmission spectrum and signal levels of the wine-glass and radial vibration modes using this differential setup. The results presented here can lead to closing the loop on a wine-glass optomechanical oscillator (OMO).

BALANCED OPTOMECHANIC SENSING

Dispersive and Reactive Optomechanical Coupling

The optomechanical system presented in this work uses two waveguides to couple to counter propagating light fields within the optical ring cavity. Therefore, the equations of motion for the intracavity field amplitudes are described by the coupled mode equations for a travelling-wave-resonator (TWR) waveguide system [5, 6]

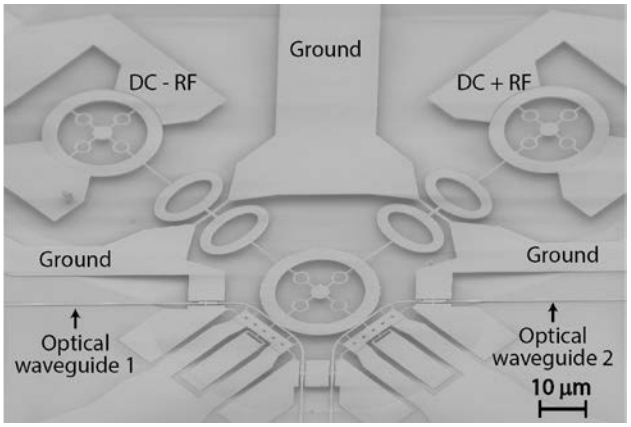

Figure 1: SEM highlighting differential electrostatic actuation and dual-waveguide differential optomechanical displacement sensing.

$$\dot{a}_{cw} = i\Delta(x)a_{cw} - \frac{\kappa}{2}a_{cw} + i\mu a_{ccw} + \sqrt{\kappa_{ex}(x)}s_{cw}^{in} \qquad (1)$$

$$\dot{a}_{ccw} = i\Delta(x)a_{ccw} - \frac{\kappa}{2}a_{ccw} + i\mu a_{cw} + \sqrt{\kappa_{ex}(x)}s_{ccw}^{in} \qquad (2)$$

where a_{cw} and a_{ccw} are the clockwise and counter-clockwise propagating intracavity light amplitudes. The total optical cavity decay rate can be expressed as $\kappa = \kappa_0 + \kappa_{ex,1} + \kappa_{ex,2}$ where κ_0 is the intrinsic decay rate of the optical cavity, and $\kappa_{ex,i}$ is the coupling rate between the optical cavity and waveguide $(i = 1,2)$. The cross coupling term μ is a function of the scattering present in the ring [5]. The optical fields are described such that $|a_i|^2$ is normalized to the intracavity energy and $\left|s_i^{in}\right|^2$ is normalized to the input power (P_{in}). These coupled mode equations are set in the rotating reference frame of the input laser frequency $(s_i^{in}(t) = s_i^{in}e^{i\omega t})$ [6].

These TWR-waveguide coupled mode equations also describe the coupling to the mechanical harmonic oscillator. The optomechanical coupling mechanisms can be classified as either dispersive or reactive [7, 8]. Dispersive coupling is a shift in the optical resonance frequency as a function of the mechanical resonator's displacement. This dispersive coupling is both a function of the mechanical ring's motion itself and its motion relative to the coupling waveguide. The expansion and contraction of the ring result in a path-length change that the intracavity light sees, shifting the resonance frequency. The ring's motion relative to the waveguide also causes a change in the perturbed index for the optical mode, also resulting in a frequency shift [7, 8]. Since the dispersive

coupling due to the perturbed index change is much smaller than the path-length change, it is treated as negligible [7]. Therefore, the only dispersive optomechanical coupling examined in this work is through path-length changes.

Reactive optomechanical coupling is a result of the mechanical ring's displacement altering the coupling rate between the optical cavity and waveguide. Therefore, the dispersive coupling $\Delta(x)$ and reactive coupling $\sqrt{\kappa_{ex}(x)}$ terms in the optical coupled mode equations can be linearized for small harmonic mechanical displacements. Also, to simplify the analysis of this two waveguide system, the scattering is assumed negligible such that $\mu = 0$. This decouples the intracavity mode equations and results in a first order differential equation describing the field amplitude for each waveguide. In this setup, waveguide 1 operates with the clockwise propagating field $\{i = 1,cw\}$ and waveguide 2 operates with the counter-clockwise field $\{i = 2,ccw\}$. For balanced detection, the coupling points of both waveguides must be similar such that $\kappa_{ex,1} = \kappa_{ex,2} = \kappa_{ex}$. The expanded intracavity field equation for each waveguide is

$$\dot{a}_i = i\big(\Delta + g_{om}x_p\big)a_i - \frac{\kappa}{2}a_i + \left(\sqrt{\kappa_{ex}} + \frac{\gamma_{om}x_i}{2\sqrt{\kappa_{ex}}}\right)s_i^{in} \quad (3)$$

With an input laser frequency of ω, the detuning from the cavity resonance is given as $\Delta = \omega - \omega_0$. The dispersive coupling coefficient for the optical ring's path-length change is defined as $g_{om} = -\partial\omega_0/\partial x_p$ where the effective radial displacement x_p of the mechanical mode is determined by integrating the displacement profile of the mode $x(\theta)$ around the ring, $x_p = 1/2\pi \oint x(\theta)\, d\theta$. This effective radial displacement is what contributes to the optical path-length change. The reactive coupling coefficient for the gap-change is defined as $\gamma_{om} = \partial\kappa_{ex}/\partial x_i$ where x_i is the displacement of the mechanical mode at the coupling point of each waveguide, which can be found by evaluating the displacement profile at each coupling point $x_i = x(\theta_i)$.

Intensity Modulation Displacement Detection

The mechanical displacement is detected through the intensity modulation of the intracavity light field. The intracavity field for each waveguide can be found through perturbation analysis with similar treatment found in [6]. A first order approximation of the field amplitude can be expressed as $a_i(t) = a_i^{(0)}(t) + a_i^{(1)}(t)$ where $a_i^{(0)}(t)$ is the steady-state field amplitude at the laser frequency ω and $a_i^{(1)}(t)$ is the modulated intracavity field. Assuming time harmonic motion of the mechanical displacement $x(t) = x\cos(\Omega_m t)$ the modulated field will comprise of two frequency components, an upshifted anti-Stokes sideband $(\omega + \Omega_m)$ and a down shifted Stokes sideband $(\omega - \Omega_m)$ [6].

The intracavity light field is then coupled out of the optical cavity and the output light field is detected by a photodetector (PD). The output light field can be expressed as $s_i^{out} = s_i^{in} - \sqrt{\kappa_{ex}(x)}a_i$ where the output field $|s_i^{out}|^2$ is normalized to the light's power at the output of the waveguide. This output coupling is again a function of the reactive optomechanical coupling and can be linearized as

$$s_i^{out} = s_i^{in} - \left(\sqrt{\kappa_{ex}} + \frac{\gamma_{om}x_i}{2\sqrt{\kappa_{ex}}}\right)a_i \quad (4)$$

To determine the nature of the modulation picked up by the PD, the output light field must also be treated through perturbation analysis such that the output field for each waveguide is $s_i^{out}(t) = s_i^{out(0)}(t) + s_i^{out(1)}(t)$. The voltage output of each PD is proportional to the optical power of the output field. The resulting voltage signal has two frequency components, a DC component from the steady-state output field and a Ω_m component from the sum of the Stokes and anti-Stokes sideband amplitudes. The PD output voltage at the mechanical resonance frequency can be expressed as

$$V_i^{PD}(\Omega_m, t) = 2Re\left\{s_i^{out(0)*}(t)s_i^{out(1)}(t)\right\} \quad (5)$$

This output voltage can be expressed in terms of the dispersive coupling, reactive coupling, and mechanical displacements as

$$V_i^{PD}(\Omega_m, t) = \gamma_{om}x_i\mathrm{K}_\gamma + g_{om}x_p\mathrm{K}_g \quad (6)$$

where K_γ and K_g are constants for both the reactive and dispersive coupling, respectively. For each waveguide, these constants depend on the input laser power, optical cavity resonance, optical detuning, decay rates of the optical cavity, and mechanical resonance frequency.

Differential and Common PD Signals

With identical coupling conditions for each waveguide, the output voltage for both waveguides 1 and 2 can now be either subtracted (differential) or added (common) to give the resulting voltages

$$V_{diff}^{PD}(\Omega_m, t) = \gamma_{om}(x_1 - x_2)\mathrm{K}_\gamma \quad (7)$$

$$V_{comm}^{PD}(\Omega_m, t) = \gamma_{om}(x_1 + x_2)\mathrm{K}_\gamma + 2g_{om}x_p\mathrm{K}_g \quad (8)$$

Equations (7) and (8) can be applied to any mechanical mode of the ring resonator. While the reactive coupling terms appear in both the difference and common PD signals, the dispersive coupling is inherently common mode because it is independent of waveguide placement around the resonator.

With the waveguide placement at the anti-nodes of the desired wine-glass mode, selective transduction over dispersive path-length change modes (like radial breathing mode) can be achieved. For the wine-glass mode, the displacements are 180° out of phase at the waveguide coupling points such that $x_2 = -x_1$. Also, due to the elliptical shape of the wine-glass mode, there is a negligible change in the ring's effective radius ($x_p \approx 0$). This results in a signal

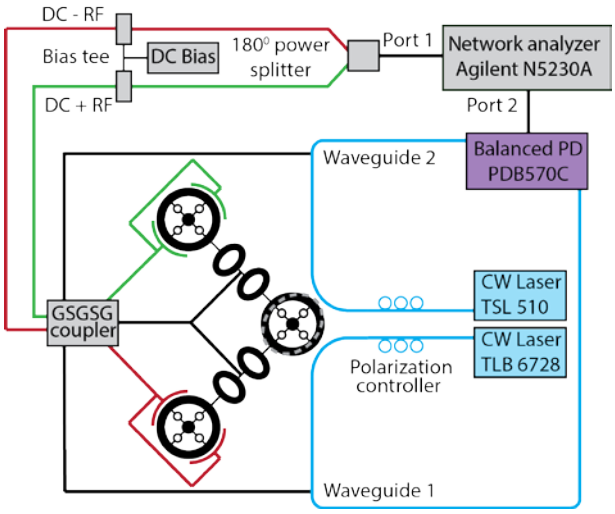

Figure 2: Fully differential experimental setup. Blue lines are the optical waveguides, red/green lines are the RF drive signals, and black lines are ground.

almost entirely due to reactive coupling and can achieve a 2x enhancement in PD voltage (6 dB increase in power) through differential detection.

Mechanical modes dominated by dispersive coupling, like the radial mode, with equal displacements at both coupling points ($x_2 = x_1$) result in a voltage output almost entirely common mode and a minimal (attenuated) differential signal.

RESONATOR DESIGN

The silicon resonator presented in this work is fabricated on a silicon-on-insulator (SOI) platform similar to the work presented in [1]. This device, however, was fabricated with a two mask process on a (100) orientated SOI stack with a high resistivity (10-20 ohm-cm) silicon device layer of 220 nm and 3 µm BOX layer. The first mask (defining the device layer) was patterned using e-beam lithography while the second mask was used to define the release region. Figure 1 shows an SEM of the fabricated device. The rings have an outer radius of 15 µm, inner radius of 11.3 µm, and four circle spokes with radius 1.8 µm. The electrode-ring gaps are 100 nm and the waveguide-ring gaps are 100 nm.

To reduce optical losses from the electrostatics, a coupled ring architecture was implemented. The displacement of the electrostatically actuated rings are coupled to the optical ring through a dumbbell coupling beam because a traditional λ/2 coupling beam was too long to practically implement in this system at 22MHz. The coupling beam was designed to have a nodal point at the center to allow for a grounding point with minimal anchor losses. The ellipses were designed such that they had a resonant extensional mode at the wine-glass frequency (22MHz). The total coupling beam length is 49 µm with each ellipse having a major axis of 20.5 µm and a minor axis of 12.5 µm. Since this coupling beam was designed for the wine-glass mode, it is less efficient in coupling the displacements of the higher frequency radial modes.

EXPERIMENTAL SETUP

Differential electrostatic drive was implemented through two orthogonal rings coupled to the optical ring and driven 180° out of phase. This driving scheme favorably excites the 22 MHz wine-glass mode over the radial mode since the latter requires in phase electrostatic drive.

Figure 2 shows the schematic of the two RF electrodes and two sense waveguides placed in-line with the out of phase anti-node pairs of the 22 MHz wine-glass mode (displacement profile shown as dashed grey line). The electrodes are driven with DC-biased RF signals to excite the ring. The ring, which is also an optical cavity, is pumped with optical power using two 1550nm lasers detuned from a different optical resonance in each waveguide. Two different optical resonances are needed to avoid interference effects within the optical cavity. The detuning and input laser power in each waveguide were adjusted so that the signal power from the PD's was balanced. By exploiting the fact that both waveguides will see identical "path-length" change but differential gap-changes, we selectively measure higher modulation from the 22 MHz wine-glass mode.

RESULTS

Figures 3 and 4 show the transmission spectrum of the optomechanical resonator with the wine-glass mode at 22 MHz and the radial mode at 96.2 MHz. While these modes have a mechanical Q (in air and room temperature) of 330 and 1,250, respectively, high Q wine-glass modes have been demonstrated and measured in vacuum [9]. The optical resonance of interest has a loaded optical quality factor of 35,000. RF transmission measurements are performed for both waveguide 1 (blue) and waveguide 2 (red) to examine the transduction of the wine-glass and radial modes with single ended optomechanical sensing. These are then compared with the fully differential sensing scheme (black).

The single ended measurement of the wine-glass mode shows a signal level close to -76 dB and the radial mode with a signal level of -94 dB. Even with the single ended measurement, the wine-glass mode is 18 dB above the radial mode. This selectivity is a result of the mechanical coupling beam design and differential electrostatic drive both favoring transduction of the wine-glass mode.

Since the two waveguide signals are almost 180° out of phase for the wine-glass mode, figure 3 shows a 5.4 dB enhancement of the signal, which is almost as high as the maximum possible differential gain in power (6 dB). Since the maximum signal enhancement is 2x (3 dB) the single ended PD voltage, then that results in a 6 dB enhancement of the signal power (~V^2). In figure 4, however, the two waveguide signals are in phase and have a large path-length contribution for the radial mode, which leads to an 11 dB attenuation in the differential signal compared to the single ended measurement. With the inclusion of differential optomechanical sensing, the wine-glass mode is now 34.4 dB above the radial mode (a 16.4 dB improvement in sensitivity from single ended measurement). The enhancement and attenuation of each mode is summarized in table 1.

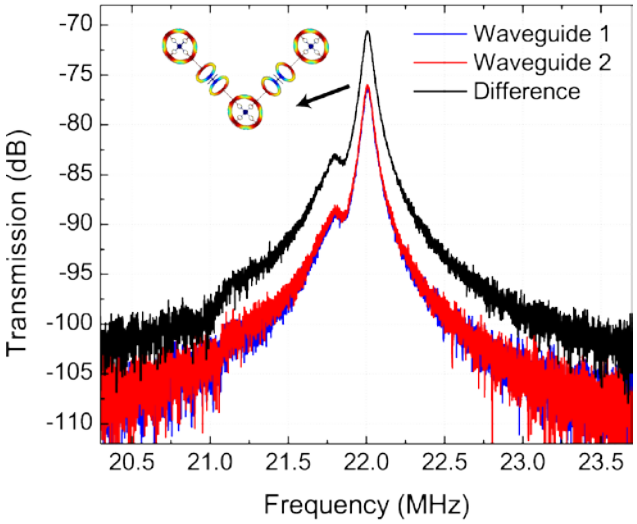

Figure 3: RF transmission of wine-glass vibration mode. P_{RF}=8 dBm, V_{DC}=13 V, λ_1=1566.45 nm, λ_2=1574.837 nm, P_{opt}=6 dBm. Difference shows enhancement of 5.4 dB

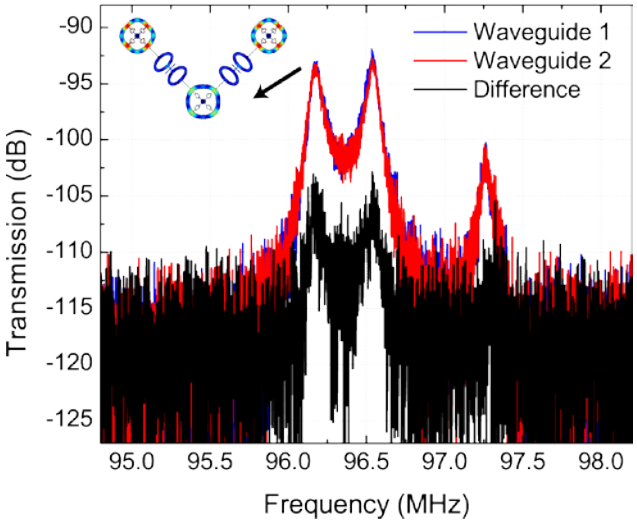

Figure 4: RF transmission of radial vibration mode. Measurement taken with the exact same experiment settings as figure 3. Difference shows attenuation of 11 dB

CONCLUSION

This is the first demonstration of the wine-glass mode being the dominant mode without the use of external filters. The theory behind dispersive and reactive optomechanical coupling was investigated for a two waveguide differential displacement sensing scheme. Using a 3-coupled ring design, fully differential electrostatic drive and differential optical sensing was implemented. With differential sensing, (compared to single ended optomechanical sensing), a 5.4 dB enhancement was obtained in the desired wine-glass mode and an 11 dB attenuation of the common radial mode was realized. The differential optomechanical sensing scheme can, for example, be adapted for high frequency wine-glass mode optomechanical oscillators (OMO). In total, the 34.4 dB higher attenuation of the radial mode allows for a simple gain stage to be used for sustaining wine-glass mode oscillations. Another application is for wine-glass vibratory gyroscopes by driving one wine-glass mode and selectively measuring the orthogonal wine-glass (Coriolis) mode.

ACKNOWLEDGEMENTS

We would like to thank Dr. Renyuan Wang for help with the theory, Prof. Mukund Vengalattore for inputs on the optical measurements, and Dr. Suresh Sridaran for his insights towards data interpretation.

Table 1: Comparison of the wine-glass mode enhancement and radial mode attenuation with differential detection.

Resonant Mode	Signal Phase Difference	Differential Signal	Balanced Output
Wine-glass (Fig. 3)	180°	**5.4 dB** Enhanced	**-70.5 dB**
Radial (Fig. 4)	0°	**11 dB** Attenuated	**-104.9 dB**

REFERENCES

[1] S. Sridaran et al., "Opto-acoustic oscillator using silicon MEMS optical modulator," in *16th International Conference on Solid-State Sensors, Actuators and Microsystems (Transducers'11)*, pp. 2920-2923.

[2] T. Beyazoglu et al., "A multi-material Q-boosted low phase noise optomechanical oscillator," in *Proceedings of IEEE MEMS 2014*, pp. 1193-96.

[3] S. Tallur and S. Bhave, "Comparison of f-Q scaling in wineglass and radial modes in ring resonators," in *Proceedings of IEEE MEMS 2013*, pp. 777-780.

[4] T. T. Fricke et al., "DC readout experiment in Enhanced LIGO," *Classical and Quantum Gravity*, vol. 29, no. 6, p. 065005, Mar. 2012.

[5] T. J. Kippenberg, S. M. Spillane, and K. J. Vahala, "Modal coupling in traveling-wave resonators," *Optics Letters*, vol. 27, no. 19, p. 1669, Oct. 2002.

[6] M. Aspelmeyer, T. J. Kippenberg, and F. Marquardt, "Cavity optomechanics," *Reviews of Modern Physics*, vol. 86, no. 4, pp. 1391-1452, Dec. 2014.

[7] M. Li, W. H. P. Pernice, and H. X. Tang, "Reactive Cavity Optical Force on Microdisk-Coupled Nanomechanical Beam Waveguides," *Physical Review Letters*, vol. 103, no. 22, p. 223901, Nov. 2009.

[8] G. Anetsberger et al., "Cavity optomechanics and cooling nanomechanical oscillators using microresonator enhanced evanescent near-field coupling," *Comptes Rendus Physique*, vol. 12, no. 910, pp. 800-816, Dec. 2011.

[9] A. K. Bhat, M. J. Storey and S. A. Bhave, "Optomechanical sensing of wine-glass modes of a BAW resonator," *IEEE International Symposium on Inertial Sensors and Systems (ISISS 2015)*, pp. 99-100.

CONTACT

*M.J. Storey, tel: +1-847-6527140; mjs636@cornell.edu